

Unveiling the $a_0(1710)$ nature in the process $J/\psi \rightarrow \bar{K}^0 K^+ \rho^-$

Yan Ding,¹ En Wang,^{1,2,*} De-Min Li,^{1,†} Li-Sheng Geng,^{3,4,5,6,‡} and Ju-Jun Xie^{6,7,8,§}

¹*School of Physics, Zhengzhou University, Zhengzhou 450001, China*

²*Guangxi Key Laboratory of Nuclear Physics and Nuclear Technology, Guangxi Normal University, Guilin 541004, China*

³*School of Physics, Beihang University, Beijing 102206, China*

⁴*Beijing Key Laboratory of Advanced Nuclear Materials and Physics, Beihang University, Beijing, 102206, China*

⁵*Peng Huanwu Collaborative Center for Research and Education, Beihang University, Beijing 100191, China*

⁶*Southern Center for Nuclear-Science Theory (SCNT), Institute of Modern Physics, Chinese Academy of Sciences, Huizhou 516000, Guangdong Province, China*

⁷*Institute of Modern Physics, Chinese Academy of Sciences, Lanzhou 730000, China*

⁸*School of Nuclear Sciences and Technology, University of Chinese Academy of Sciences, Beijing 101408, China*
(Dated: July 25, 2024)

We have investigated the process $J/\psi \rightarrow \bar{K}^0 K^+ \rho^-$ by taking into account the S -wave $K^* \bar{K}^*$, $\rho\omega$, and $\rho\phi$ final-state interactions, where the scalar meson $a_0(1710)$ is generated. In addition, we also take into account the contributions from the scalar $a_0(980) (\rightarrow \bar{K}^0 K^+)$ and the intermediate resonances $K_1(1270)^- (\rightarrow \bar{K}^0 \rho^-)$ and $K_1(1270)^0 (\rightarrow K^+ \rho^-)$. Our results show that, in the $\bar{K}^0 K^+$ invariant mass distribution, a clear peak structure around 1.8 GeV appears, which could be associated with the scalar $a_0(1710)$, however, no significant structure of the $a_0(980)$ is observed. On the other hand, one can find clear peaks of the $K_1(1270)$ in the $\bar{K}^0 \rho^-$ and $K^+ \rho^-$ invariant mass distributions. The future precise measurement of this process by the BESIII and Belle II Collaborations and the planned Super Tau-Charm Facility (STCF) in the future could shed light on the nature of $a_0(1710)$.

I. INTRODUCTION

In the last two decades, many states have been accumulated experimentally whose properties cannot be well described by the $q\bar{q}$ mesons and the qqq baryons within the conventional quark model. Some exotic explanations are proposed for their nature, such as tetraquark, pentaquark, hybrid, glueball, kinematic effects, and the mixing of different components [1–7]. It is difficult to distinguish between those explanations, especially for states with the quantum numbers allowed by the conventional quark model [6, 7].

Recently, the *BABAR* Collaboration reported the scalar resonance $a_0(1710)$ in the $\pi^\pm \eta$ invariant mass spectrum of the process $\eta_c \rightarrow \eta \pi^\pm \pi^-$ [8]. The $a_0(1710)$ state was also observed by the BESIII Collaboration in the $K_S^0 K_S^0$ invariant mass spectrum of the process $D_s^+ \rightarrow K_S^0 K_S^0 \pi^+$ [9] and in the $K_S^0 K^+$ invariant mass spectrum of the process $D_s^+ \rightarrow K_S^0 K^+ \pi^0$ [10]. We have tabulated the experimental masses and widths of $a_0(1710)$ in Table I. It should be noted that, in Ref. [9], BESIII did not distinguish between the $a_0(1710)$ and $f_0(1710)$ in the process $D_s^+ \rightarrow K_S^0 K_S^0 \pi^+$, and denoted the combined state as $S(1710)$, while in Ref. [10] the $a_0(1710)$ was renamed as $a_0(1817)$ because of the different fitted Breit-Wigner mass of this state.

Before the observation of $a_0(1710)$, there have been

TABLE I. Experimental measurements on the mass ($M_{a_0(1710)}$) and width ($\Gamma_{a_0(1710)}$) of the scalar state $a_0(1710)$. The first error is statistical, and the second one is systematic. All values are in units of MeV.

Collaboration	$M_{a_0(1710)}$	$\Gamma_{a_0(1710)}$	Ref.
<i>BABAR</i>	$1704 \pm 5 \pm 2$	$110 \pm 15 \pm 11$	[8]
BESIII	$1723 \pm 11 \pm 2$	$140 \pm 14 \pm 4$	[9]
BESIII	$1817 \pm 8 \pm 20$	$97 \pm 22 \pm 15$	[10]

many theoretical studies about the $a_0(1710)$ and its isospin partner $f_0(1710)$ from various perspectives [11–25]. In Refs. [26, 27], the $f_0(1710)$, as a well-established state according to the Review of Particle Physics (RPP) [28], could be dynamically generated from the vector-vector interactions, and one isovector scalar state a_0 with a mass around 1770 MeV was also predicted, the picture of which remains essentially the same when the pseudoscalar-pseudoscalar coupled channels were taken into account [29]. Based on the SU(6) spin-flavor symmetry, the $f_0(1710)$ is mostly a $K^* \bar{K}^*$ bound state, and an a_0 state with a pole position of $\sqrt{s_R} = (1760, -12)$ MeV was predicted to couple strongly to $K^* \bar{K}^*$ and $\phi \rho$ in Ref. [17]. In addition, a scalar state a_0 with a mass of 1744 MeV is also predicted in the approach of the Regge trajectories [30]. In Ref. [19], it was suggested that the $f_0(1710)$ wave function contains a large $s\bar{s}$ component, while in Refs. [20–23], the $f_0(1710)$ was regarded as the candidate of a scalar glueball. Recently, it was shown that the $a_0(1710)$ as a $K^* \bar{K}^*$ molecule plays an important role in the three-body inter-

* wangen@zzu.edu.cn

† lidm@zzu.edu.cn

‡ lisheng.geng@buaa.edu.cn

§ xiejujun@impcas.ac.cn

actions of $\eta K^* \bar{K}^*$, which could dynamically generate the $\pi(2070)$ [31].

As shown in Table I, there is not yet a consensus on the mass of the $a_0(1710)$ experimentally, which could complicate understanding its nature. For instance, $a_0(1710)$ [or $a_0(1817)$] and $X(1812)$ have been explained as the 3^3P_0 $q\bar{q}$ state by assuming $a_0(980)$ and $f_0(980)$ as 1^3P_0 $q\bar{q}$ states [32]. However, $X(1812)$ was observed in the process $J/\psi \rightarrow \gamma\phi\omega$ by the BESIII Collaboration [33, 34], and the enhancement near the $\phi\omega$ threshold, associated with $X(1812)$, could be described by the reflection of $f_0(1710)$, as discussed in Ref. [15]. Regarding the $a_0(1710)$ as a $K^* \bar{K}^*$ molecular state, Refs. [35–39] have successfully described the invariant mass distributions of the processes $D_s^+ \rightarrow K_S^0 K_S^0 \pi^+$ and $D_s^+ \rightarrow K_S^0 K^+ \pi^0$ measured by the BESIII Collaboration [9, 10].

Since the peak positions of the $a_0(1710)$ in the $K\bar{K}$ invariant mass distributions of the processes $D_s^+ \rightarrow K_S^0 K_S^0 \pi^+$, $K_S^0 K^+ \pi^0$ observed by the BESIII Collaboration are very close to the boundary region of the $K\bar{K}$ invariant mass, we have suggested to measure its properties in the process $\eta_c \rightarrow \bar{K}^0 K^+ \pi^-$ in Ref. [40], and predicted a dip structure around 1.8 GeV, associated with the $a_0(1710)$, in the $\bar{K}^0 K^+$ invariant mass distribution [40], which is consistent with the *BABAR* measurements [41]. In addition, the photoproduction process is also proposed to search for the $a_0(1710)$ in Ref. [42].

The BESIII Collaboration has accumulated $(10.09 \pm 0.04) \times 10^9$ J/ψ events at the BEPCII collider [43], and the Super Tau-Charm Facility (STCF) project under development in China is expected to accumulate 3.4×10^{12} J/ψ events per year [44]. Since the dominant decay mode of the $a_0(1710)$ state is $K\bar{K}$ within the molecular picture [26, 29], it is natural to search for the scalar $a_0(1710)$ in the process $J/\psi \rightarrow a_0(1710)^+ \rho^- \rightarrow \bar{K}^0 K^+ \rho^-$. It should be stressed that the *BABAR* Collaboration has measured this process, and the branching fraction is $\mathcal{B}(J/\psi \rightarrow K_S^0 K^\pm \rho^\mp) = (1.87 \pm 0.18 \pm 0.34) \times 10^{-3}$ [45]. However, the $K_S^0 K^\pm$ mass spectrum was not reported by the *BABAR* Collaboration [45].

In this work, we will investigate the process $J/\psi \rightarrow a_0(1710)^+ / a_0(980)^+ \rho^- \rightarrow \bar{K}^0 K^+ \rho^-$ by considering the contributions from the intermediate resonances $a_0(1710)$ and $a_0(980)$. It should be pointed out that another state $a_2(1700)$ with a mass of 1706 ± 14 MeV and a width of 378_{-50}^{+60} MeV may give a broad contribution and should not significantly affect the narrow peak of $a_0(1710)$ in the $\bar{K}^0 K^+$ invariant mass distribution [28]. Furthermore, $a_2(1700)$ couples to $K\bar{K}$ in the D wave with a small branching fraction of $\mathcal{B}(a_2(1700) \rightarrow K\bar{K}) = (1.3 \pm 0.8)\%$. Therefore, we will neglect its contribution.

On the other hand, the interactions of vector mesons and pseudoscalar mesons within the unitary chiral approach could dynamically generate the resonance $K_1(1270)$ with a two-pole structure [46–48], where the lower pole mainly couples to the $K^* \pi$ channel, and the higher one couples strongly to the $K\rho$ channel. Thus, we also consider the contribution from the intermediate

resonance $K_1(1270)$ in this work. Considering that the branching ratios of the process $K_1(1400) \rightarrow K\rho$ and $K^*(1410) \rightarrow K\rho$ are $(3.0 \pm 3.0)\%$ and $< 7\%$, which are 10 times smaller than the $\mathcal{B}(K_1(1270) \rightarrow K\rho) = (38 \pm 13)\%$ [28], we will also neglect the contributions from the intermediate states $K_1(1400)$ and $K^*(1410)$ in this work. Thus, the precise measurements of the process $J/\psi \rightarrow \bar{K}^0 K^+ \rho^-$ could also shed light on the two-pole structure of $K_1(1270)$, which is crucial to understanding the hadron-hadron interactions [49, 50].

The paper is organized as follows. In Sec. II, we present the theoretical formalism for studying the $J/\psi \rightarrow \bar{K}^0 K^+ \rho^-$ decay, and in Sec. III, we show our numerical results and discussions, followed by a summary in the last section.

II. FORMALISM

First, we present the theoretical formalism for studying the process $J/\psi \rightarrow \bar{K}^0 K^+ \rho^-$ via the $K^* \bar{K}^*$, $\omega\rho$, and $\phi\rho$ final-state interactions in coupled channels, which will generate the scalar resonance $a_0(1710)$ in Sec. II A. Next, we show the formalism for the process $J/\psi \rightarrow K_1(1270)^- K^+ [K_1(1270)^0 \bar{K}^0]$ with $K_1(1270)^- \rightarrow \bar{K}^0 \rho^-$ [$K_1(1270)^0 \rightarrow K^+ \rho^-$] in Sec. II B. In the Sec. II C, we will describe the contribution from the S -wave $K\bar{K}$ final-state interaction, which would generate the scalar meson $a_0(980)$. At last, the formalism of the double differential widths for this process is given in Sec. II D.

A. Mechanism for the intermediate $a_0(1710)$

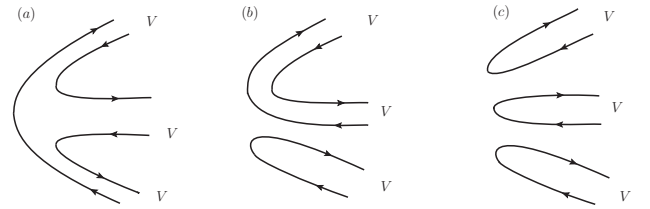


FIG. 1. Diagrammatic expression of (a) $\langle VVV \rangle$, (b) $\langle VV \rangle \langle V \rangle$, (c) $\langle V \rangle \langle V \rangle \langle V \rangle$ terms in Eq. (1).

As done in Refs. [35, 36, 40], the scalar meson $a_0(1710)$ is regarded as a vector-vector molecular state [26, 27]. To study the role of $a_0(1710)$ in the $J/\psi \rightarrow \rho^- K^+ \bar{K}^0$ decay, one needs to first produce the meson ρ^- and a vector-vector pair, then the final-state interactions of the vector-vector pair will produce the $a_0(1710)$, which decays into $K^+ \bar{K}^0$ in the final state. Considering that the J/ψ is a flavor singlet, we could introduce the combination modes in the primary vertex [51–53], whose diagrammatic expression is depicted in Fig. 1,

$$\langle VVV \rangle, \quad \langle VV \rangle \langle V \rangle, \quad \langle V \rangle \langle V \rangle \langle V \rangle, \quad (1)$$

where V is the matrix of the SU(3) vector mesons [52–54],

$$V = \begin{pmatrix} \frac{\rho^0}{\sqrt{2}} + \frac{\omega}{\sqrt{2}} & \rho^+ & K^{*+} \\ \rho^- & -\frac{\rho^0}{\sqrt{2}} + \frac{\omega}{\sqrt{2}} & K^{*0} \\ K^{*-} & \bar{K}^{*0} & \phi \end{pmatrix}, \quad (2)$$

where the symbol $\langle \dots \rangle$ stands for the trace of the SU(3) matrices. Since no term contains ρ^- in $\langle V \rangle \langle V \rangle \langle V \rangle$, we do not take this combination in our work. One could obtain the relevant contributions by isolating the terms containing ρ^- , as follows:

$$\langle VVV \rangle : \alpha \times \left[\frac{\rho^+ \rho^0}{\sqrt{2}} + 3\sqrt{2}\omega\rho^+ + 3\bar{K}^{*0}K^{*+} \right] \rho^- \quad (3)$$

$$\langle VV \rangle \langle V \rangle : \beta \times \left[2\sqrt{2}\omega\rho^+ + 2\phi\rho^+ \right] \rho^-. \quad (4)$$

Here, two parameters α and β are introduced to account for the weights of $\langle VVV \rangle$ and $\langle VV \rangle \langle V \rangle$ structures, respectively. It is concluded in Refs. [26, 55, 56] that the $\langle VVV \rangle$ one was favored and the best ratio $\beta/\alpha = 0.32$ was obtained by fitting to the experimental measurements of the process $J/\psi \rightarrow \phi VV$ [26, 56], thus we will use this finding and take $\alpha = 1$ and $\beta = 0.32$ in this work.

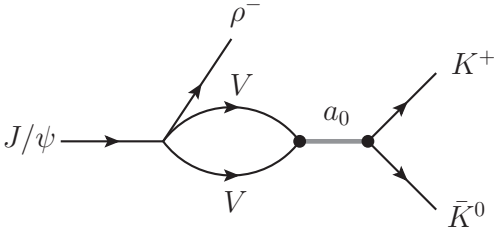


FIG. 2. Diagram for the process $J/\psi \rightarrow VV\rho^- \rightarrow a_0(1710)^+\rho^- \rightarrow K^+\bar{K}^0\rho^-$, where VV stands for $\bar{K}^{*0}K^{*+}$, $\omega\rho^+$, and $\phi\rho^+$.

In the molecular picture, the $a_0(1710)$ is dynamically generated from the S -wave $K^*\bar{K}^*$, $\omega\rho$, and $\phi\rho$ interactions in coupled channels [26, 27]¹, and then decays into the final state \bar{K}^0K^+ , as depicted in Fig. 2. The decay amplitude of Fig. 2 can be written as,

$$\begin{aligned} \mathcal{M}_a = & V_p \times [3\alpha G_{\bar{K}^{*0}K^{*+}} t_{\bar{K}^{*0}K^{*+} \rightarrow \bar{K}^0K^+} \\ & + (2\sqrt{2}\beta + 3\sqrt{2}\alpha) G_{\omega\rho^+} t_{\omega\rho^+ \rightarrow \bar{K}^0K^+} \\ & + 2\beta G_{\phi\rho^+} t_{\phi\rho^+ \rightarrow \bar{K}^0K^+}], \end{aligned} \quad (5)$$

where V_p is a global factor, and $t_{\bar{K}^{*0}K^{*+} \rightarrow \bar{K}^0K^+}$, $t_{\omega\rho^+ \rightarrow \bar{K}^0K^+}$, and $t_{\phi\rho^+ \rightarrow \bar{K}^0K^+}$ are the transition amplitudes. $G_{\bar{K}^{*0}K^{*+}}$, $G_{\omega\rho^+}$, and $G_{\phi\rho^+}$ are the loop functions

for the $\bar{K}^{*0}K^{*+}$, $\omega\rho^+$, and $\phi\rho^+$ channels, respectively, and read [26, 57],

$$G_i(M_{\bar{K}^0K^+}) = \int_{m_{1-}^2}^{m_{1+}^2} \int_{m_{2-}^2}^{m_{2+}^2} d\tilde{m}_1^2 d\tilde{m}_2^2 \times \omega(\tilde{m}_1^2) \omega(\tilde{m}_2^2) \tilde{G}(M_{\bar{K}^0K^+}, \tilde{m}_1^2, \tilde{m}_2^2), \quad (6)$$

where

$$\omega(\tilde{m}_i^2) = \frac{1}{N} \left(-\frac{1}{\pi} \right) \text{Im} \left[\frac{1}{\tilde{m}_i^2 - m_{V_i}^2 + i\Gamma(\tilde{m}_i^2)\tilde{m}_i} \right], \quad (7)$$

$$N = \int_{\tilde{m}_{i-}^2}^{\tilde{m}_{i+}^2} d\tilde{m}_i^2 \left(-\frac{1}{\pi} \right) \text{Im} \left[\frac{1}{\tilde{m}_i^2 - m_{V_i}^2 + i\Gamma(\tilde{m}_i^2)\tilde{m}_i} \right], \quad (8)$$

$$\Gamma(\tilde{m}_i^2) = \Gamma_{V_i} \frac{\tilde{k}^3}{k^3} \Theta(\tilde{m} - m_{P_1} - m_{P_2}), \quad (9)$$

$$\tilde{k} = \frac{\lambda^{\frac{1}{2}}(\tilde{m}_i^2, m_{P_1}^2, m_{P_2}^2)}{2\tilde{m}_i}, \quad k = \frac{\lambda^{\frac{1}{2}}(m_{V_i}^2, m_{P_1}^2, m_{P_2}^2)}{2m_{V_i}}, \quad (10)$$

with the Källén function $\lambda(x, y, z) = x^2 + y^2 + z^2 - 2xy - 2xz - 2yz$. Here, we consider the decay channels $\pi\pi$ and $K\pi$ for the vector mesons ρ and K^* , respectively, and neglect the small widths of ω ($\Gamma_\omega = 8.68$ MeV) and ϕ ($\Gamma_\phi = 4.249$ MeV). Taking the vector K^* for example, $m_{1+}^2 = (m_{K^*} + 2\Gamma_{K^*})^2$ and $m_{1-}^2 = (m_{K^*} - 2\Gamma_{K^*})^2$. Similarly, one can obtain m_{1+}^2 and m_{1-}^2 for the ρ meson. The masses, widths, and spin parities of the involved particles are taken from the RPP [28], as listed in Table II.

TABLE II. Masses, widths, and spin-parities of the involved particles in this work. All values are in units of MeV.

State	Mass	Width	Spin parity (J^P)
J/ψ	3096.900	0.0926	1^-
$\rho^{\pm,0}$	775.26	149.1	1^-
\bar{K}^0	497.611	-	0^-
K^\pm	493.677	-	0^-
K^*	893.6	49.1	1^-
ω	782.66	8.68	1^-
ϕ	1019.461	4.249	1^-
$K_1(1270)$	1284	146	1^+

The loop function \tilde{G} in Eq. (6) is for stable particles, and in the dimensional regularization scheme, it can be written as [58],

$$\begin{aligned} \tilde{G} = & \frac{1}{16\pi^2} \left\{ a_\mu + \ln \frac{m_1^2}{\mu^2} + \frac{m_2^2 - m_1^2 + s}{2s} \ln \frac{m_2^2}{m_1^2} \right. \\ & \frac{p}{\sqrt{s}} \left[\ln(s - (m_2^2 - m_1^2) + 2p\sqrt{s}) \right. \\ & + \ln(s + (m_2^2 - m_1^2) + 2p\sqrt{s}) \\ & - \ln(-s + (m_2^2 - m_1^2) + 2p\sqrt{s}) \\ & \left. \left. - \ln(-s - (m_2^2 - m_1^2) + 2p\sqrt{s}) \right] \right\}, \end{aligned} \quad (11)$$

¹ It should be noted that, the conservation of G parity forbids the coupling of $a_0(1710)$ to the channel $\rho\rho$.

with

$$p = \frac{\lambda^{1/2}(s, m_1^2, m_2^2)}{2\sqrt{s}}, \quad (12)$$

where a_μ is the subtraction constant, μ is the dimensional regularization scale, and $s = M_{\bar{K}^0 K^+}^2$. In this work, we take $a_\mu = -1.726$ and $\mu = 1000$ MeV as used in Ref. [26]. It is worth mentioning that any change in μ could be re-absorbed by a change in a_μ through $a_{\mu'} - a_\mu = \ln(\mu'^2/\mu^2)$, which implies that the loop function \tilde{G} is scale independent [59].

To show the influence of the widths of vector mesons on the loop functions, we have calculated the loop functions $G_{\phi\rho^+}$ and $\tilde{G}_{\phi\rho^+}$ as functions of the $\bar{K}^0 K^+$ invariant mass,² as presented in Fig. 3. The blue dashed and red dot-dashed curves correspond to the real and imaginary parts of the loop function G , considering the width of ρ . In contrast, the green solid and purple dotted curves correspond to the real and imaginary parts of the loop function \tilde{G} without the contribution from the ρ width, respectively. One can find that the loop functions G , considering the width of the vector meson, become smoother around the threshold of the $\phi\rho$.

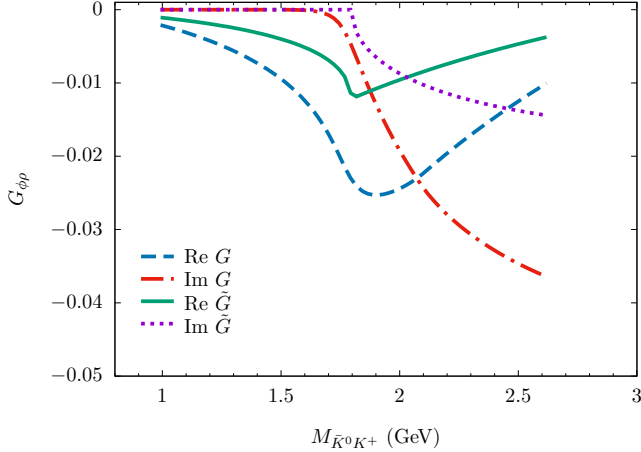


FIG. 3. Real and imaginary parts of the loop functions $G_{\phi\rho}$ and $\tilde{G}_{\phi\rho}$ as a function of the $\bar{K}^0 K^+$ invariant mass. The blue dashed and red dot-dashed curves correspond to the real and imaginary parts of the loop function G , considering the width of ρ . Meanwhile, the green solid and purple dotted curves correspond to the real and imaginary parts of the loop function \tilde{G} without the contribution from the ρ width, respectively.

On the other hand, the transition amplitudes $t_{i \rightarrow \bar{K}^0 K^+}$ in Eq. (5) can be written as,

$$t_{i \rightarrow \bar{K}^0 K^+} = \frac{g_i \times g_{K\bar{K}}}{M_{\bar{K}^0 K^+}^2 - M_{a_0(1710)}^2 + iM_{a_0(1710)}\Gamma_{a_0(1710)}} \quad (13)$$

² One can find the invariant mass distributions of the loop functions $\tilde{G}_{\bar{K}^* K^+}$ and $\tilde{G}_{\omega\rho}$ in Refs. [35, 40].

TABLE III. Mass, width, and coupling constants of the scalar $a_0(1710)$ [26]. All values are in units of MeV.

Parameters	Value
Mass	1777
Width	148
$\Gamma_{K\bar{K}}$	36
$g_{K\bar{K}}$	1966
$g_{\rho\rho}$	0
$g_{K^* \bar{K}^*}$	(7525, -1529)
$g_{\omega\rho}$	(-4042, 1391)
$g_{\phi\rho}$	(4998, -1872)

where $M_{a_0(1710)}$ and $\Gamma_{a_0(1710)}$ are the mass and width of the $a_0(1710)$, respectively, and we take their values from Refs. [26, 60], which are tabulated in Table III. g_i are the coupling constants of $a_0(1710)$ to $K^* \bar{K}^*$, $\omega\rho$, and $\phi\rho^+$, whose values are determined in Ref. [26], while the coupling $g_{K\bar{K}}$ is determined from the partial decay width of $a_0(1710) \rightarrow K\bar{K}$,

$$\Gamma_{K\bar{K}} = \frac{g_{K\bar{K}}^2 |\vec{p}_K|}{8\pi M_{a_0}^2}, \quad (14)$$

where \vec{p}_K is the three-momentum of the K or \bar{K} meson in the $a_0(1710)$ rest frame,

$$|\vec{p}_K| = \frac{\lambda^{1/2}(M_{a_0}^2, m_K^2, m_K^2)}{2M_{a_0}}. \quad (15)$$

With the partial decay width $\Gamma_{K\bar{K}} = 36$ MeV predicted by Ref. [26], one can only obtain the absolute value of the coupling constant, but not the phase, thus by assuming that $g_{K\bar{K}}$ is real and positive we take $g_{K\bar{K}} = 1966$ MeV, as done in Refs. [35, 36].

B. Mechanism for the intermediate $K_1(1270)$

In Fig. 4, we show the Dalitz plot for the process $J/\psi \rightarrow \bar{K}^0 K^+ \rho^-$, and one can find that the contribution from the $K_1(1270)$ (the green band) could interfere with the one from the $a_0(1710)$ (the red band) close to the $K\rho$ threshold. Since the $K_1(1270)$ state could be dynamically generated from the interaction of vector mesons and pseudoscalar mesons [46, 47], the $K^+ \rho^-$ and $\bar{K}^0 \rho^-$ could undergo the S -wave final-state interaction, which will generate the $K_1(1270)$ state, followed by the decay $K_1(1270) \rightarrow K\rho$, as depicted in Fig. 5.

The decay amplitude for $J/\psi \rightarrow \bar{K}^0 K_1(1270)^- \rightarrow \bar{K}^0 K^+ \rho^-$ of Fig. 5(a) can be written as

$$\mathcal{M}_b = V_p' \times G_{K^+ \rho^-} t_{K^+ \rho^- \rightarrow K^+ \rho^-}, \quad (16)$$

where V_p' stands for the weight of the direct production vertex, and the $t_{K^+ \rho^- \rightarrow K^+ \rho^-}$ is the transition amplitude,

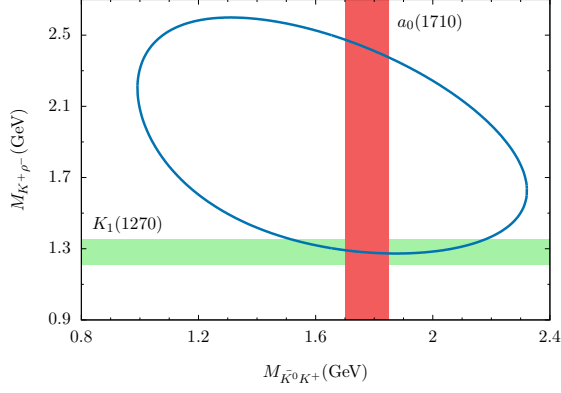


FIG. 4. The Dalitz plot for the $J/\psi \rightarrow \bar{K}^0 K^+ \rho^-$. The red band stands for the region of $M_{a_0} \pm \frac{1}{2}\Gamma_{a_0}$ where the predicted $a_0(1710)$ state lies. The green band stands for the region of $M_{K_1} \pm \frac{1}{2}\Gamma_{K_1}$ where the $K_1(1270)$ state lies.

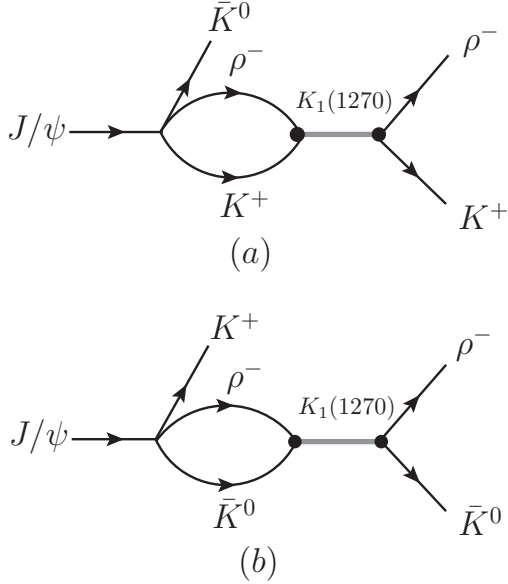


FIG. 5. Diagrams for $J/\psi \rightarrow \bar{K}^0 K^+ \rho^-$ via the intermediate (a) $K_1(1270)^0$ and (b) $K_1(1270)^-$, followed by the decay $K_1(1270)^{0,-} \rightarrow K^+ \rho^- / \bar{K}^0 \rho^-$.

which can be written as

$$t_{K^+ \rho^- \rightarrow K^+ \rho^-} = \frac{g_{K^+ \rho^-} g_{K^+ \rho^-}}{M_{K^+ \rho^-}^2 - M_{K_1}^2 + iM_{K_1} \Gamma_{K_1}}, \quad (17)$$

where $M_{K^+ \rho^-}$ is the invariant mass of the $K^+ \rho^-$ system, and $g_{K^+ \rho^-}$ denotes the coupling constant. In this work, we adopt the value $g_{K^+ \rho^-} = (4804 + i395)$ MeV of Table IV. Since the higher pole of the $K_1(1270)$ mainly couples to the $K\rho$ channel, we can relate the mass and width of the $K_1(1270)$ with the higher pole position of Table IV, i.e. $M_{K_1} = \text{Re}\sqrt{s_0}$ and $\Gamma_{K_1} = 2\text{Im}\sqrt{s_0}$. Similarly, the amplitude of the process $J/\psi \rightarrow K^+ K_1(1270)^- \rightarrow$

TABLE IV. Pole positions and coupling constants of the two poles of the $K_1(1270)$ [46]. All values are in units of MeV.

	First pole	Second pole
Pole position $\sqrt{s_0}$	$1195 - i123$	$1284 - i73$
$g_{K\rho}$	$-1671 + i1599$	$4804 + i395$

$K^+ \bar{K}^0 \rho^-$, as depicted in Fig. 5(b), can be expressed as,

$$\mathcal{M}_c = V'_p \times G_{\bar{K}^0 \rho^-} t_{\bar{K}^0 \rho^- \rightarrow \bar{K}^0 \rho^-}, \quad (18)$$

$$t_{\bar{K}^0 \rho^- \rightarrow \bar{K}^0 \rho^-} = \frac{g_{\bar{K}^0 \rho^-} g_{\bar{K}^0 \rho^-}}{M_{\bar{K}^0 \rho^-}^2 - M_{K_1}^2 + iM_{K_1} \Gamma_{K_1}}, \quad (19)$$

where $M_{\bar{K}^0 \rho^-}$ is the $\bar{K}^0 \rho^-$ invariant mass, and $g_{\bar{K}^0 \rho^-}$ is the coupling constant, $g_{\bar{K}^0 \rho^-} = g_{K^+ \rho^-} = (4804 + i395)$ MeV in this work. We take the same weight V'_p for the contributions from the $K_1(1270)^0$ and $K_1(1270)^-$.

According to Eqs. (6) and (11), we have also calculated the loop function $G_{K^+ \rho^-} / G_{\bar{K}^0 \rho^-}$ and $\tilde{G}_{K^+ \rho^-} / \tilde{G}_{\bar{K}^0 \rho^-}$ as functions of the $K^+ \rho^-$ and $\bar{K}^0 \rho^-$ invariant masses, respectively, as presented in Figs. 6 and 7. One can find that the loop functions G become smoother around the threshold when considering the width of the ρ .

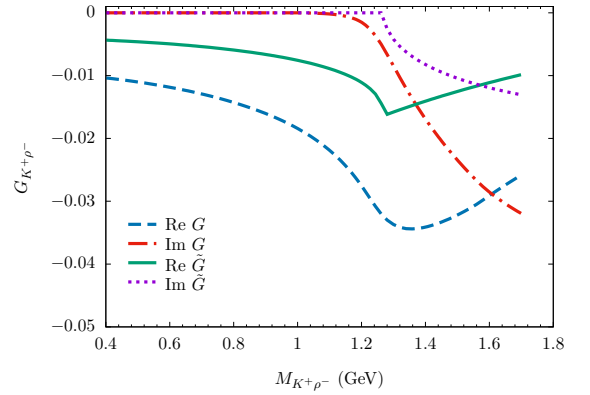


FIG. 6. Real and imaginary parts of the loop functions $G_{K^+ \rho^-}$ and $\tilde{G}_{K^+ \rho^-}$ as a function of the $K^+ \rho^-$ invariant mass. The notations of the curves are the same as those of Fig. 3.

C. Mechanism for the intermediate $a_0(980)$

In addition to the intermediate resonances $a_0(1710)$ and $K_1(1270)$, the process $J/\psi \rightarrow K^+ \bar{K}^0 \rho^-$ can happen via the direct production, as depicted in Fig. 8(a), and the $K^+ \bar{K}^0$ final-state interaction, which generates the scalar meson $a_0(980)$, as depicted in Fig. 8(b). Thus, the decay amplitude can be written as

$$\mathcal{M}_d = V'_p [1 + G_{K\bar{K}} t_{\bar{K}^0 K^+ \rightarrow \bar{K}^0 K^+}], \quad (20)$$

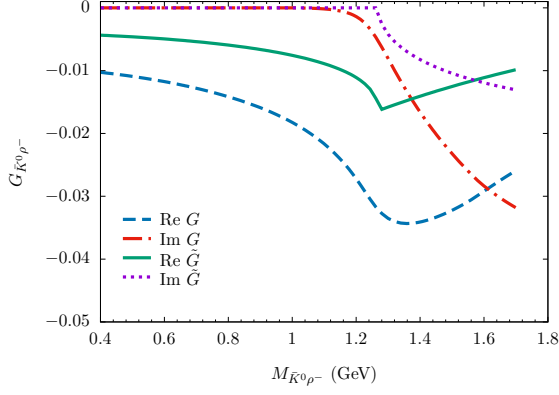


FIG. 7. Real and imaginary parts of the loop functions $G_{\bar{K}^0 \rho^-}$ and $\tilde{G}_{\bar{K}^0 \rho^-}$ as a function of the $\bar{K}^0 \rho^-$ invariant mass. The notations of the curves are the same as those of Fig. 3.

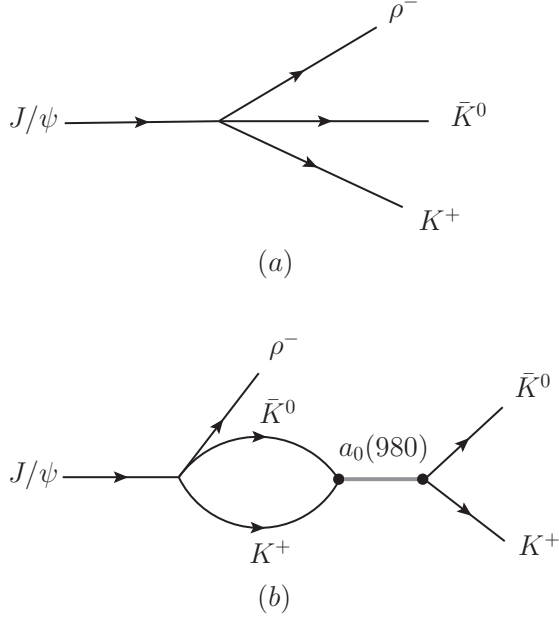


FIG. 8. Diagrams for the process $J/\psi \rightarrow a_0(980)^+ \rho^- \rightarrow K^+ \bar{K}^0 \rho^-$. (a) Tree diagram and (b) the final-state interaction of $\bar{K}^0 K^+$ to produce the $a_0(980)$ state.

where V_p' is the weight of the direct production vertex $J/\psi \rightarrow \rho^- \bar{K}^0 K^+$ of Fig. 8(a), the same as the one of Eq. (18). The loop function $G_{K\bar{K}}$ could be written as

$$G_{K\bar{K}} = i \int \frac{d^4 q}{(2\pi)^4} \frac{1}{(P-q)^2 - m_1^2 + i\epsilon} \frac{1}{q^2 - m_2^2 + i\epsilon}, \quad (21)$$

where m_1 and m_2 are the masses of the two mesons in the loop of the $K\bar{K}$ channel, and P and q are the four-momenta of the $K\bar{K}$ system and the \bar{K} meson, respectively. The loop function of Eq. (22) is logarithmically divergent. For $G_{K\bar{K}}$, we adopt the cutoff method, and

perform the integral for q in Eq. (22) with a cutoff $q_{\max} = 903$ MeV to regularize the loop, the same as Ref. [36].

The $t_{\bar{K}^0 K^+}$ is the transition amplitude, which depends on the invariant mass $M_{\bar{K}^0 K^+}$, and could be obtained in the chiral unitary approach by solving the Bethe-Salpeter equation [61–64]

$$T = [1 - VG]^{-1}V \quad (22)$$

where V is a 2×2 matrix with the transition potentials between the isospin channels $K\bar{K}$ and $\pi\eta$. The transition amplitudes $t_{\bar{K}^0 K^+ \rightarrow \bar{K}^0 K^+}$ in particle basis can be related to the one in isospin basis,

$$t_{\bar{K}^0 K^+ \rightarrow \bar{K}^0 K^+} = t_{K\bar{K} \rightarrow K\bar{K}}. \quad (23)$$

With the isospin multiplets $K = (K^+, K^0)$, $\bar{K} = (\bar{K}^0, -K^-)$, $\pi = (-\pi^+, \pi^0, \pi^-)$, the 2×2 matrix V can be easily obtained as follows [65–68]:

$$\begin{aligned} V_{K\bar{K} \rightarrow K\bar{K}} &= -\frac{1}{4f^2}s \\ V_{K\bar{K} \rightarrow \pi\eta} &= \frac{\sqrt{6}}{12f^2}(3s - \frac{8}{3}m_K^2 - \frac{1}{3}m_\pi^2 - m_\eta^2) \\ V_{\pi\eta \rightarrow K\bar{K}} &= V_{K\bar{K} \rightarrow \pi\eta} \\ V_{\pi\eta \rightarrow \pi\eta} &= -\frac{1}{3f^2}m_\pi^2, \end{aligned} \quad (24)$$

where $f = 93$ MeV is the pion decay constant, m_π and m_K are the isospin averaged masses of the pion and kaon, respectively, and s is the invariant mass squared of the pseudoscalar-pseudoscalar system.

It is worth mentioning that, since the transition amplitude of Eq. (22) is unstable in the high energy region, we should not use the model for higher invariant masses. For that purpose we take the following prescription: we evaluate $Gt(M_{\text{inv}})$ combinations up to $M_{\text{inv}} = M_{\text{cut}}$. From there on, we multiply Gt by a smooth factor to make it gradually decrease at large M_{inv} . Thus, we take [69]

$$Gt(M_{\text{inv}}) = Gt(M_{\text{cut}})e^{-\alpha(M_{\text{inv}} - M_{\text{cut}})}, \quad (25)$$

for

$$M_{\text{inv}} > M_{\text{cut}}. \quad (26)$$

In our work, we take the value $M_{\text{cut}} = 1100$ MeV and $\alpha = 0.0037 \text{ MeV}^{-1}$, as used in Ref. [69].

D. Invariant mass distributions

With the amplitudes obtained above, we can write down the total decay amplitude of $J/\psi \rightarrow \bar{K}^0 K^+ \rho^-$ as follows,

$$\mathcal{M} = \mathcal{M}_a + \mathcal{M}_b + \mathcal{M}_c + \mathcal{M}_d, \quad (27)$$

and the double differential widths of the process $J/\psi \rightarrow \bar{K}^0 K^+ \rho^-$ are

$$\frac{d^2\Gamma}{dM_{\bar{K}^0 K^+} dM_{K^+ \rho^-}} = \frac{M_{\bar{K}^0 K^+} M_{K^+ \rho^-}}{128\pi^3 m_{J/\psi}^3} |\mathcal{M}|^2, \quad (28)$$

$$\frac{d^2\Gamma}{dM_{\bar{K}^0 K^+} dM_{\bar{K}^0 \rho^-}} = \frac{M_{\bar{K}^0 K^+} M_{\bar{K}^0 \rho^-}}{128\pi^3 m_{J/\psi}^3} |\mathcal{M}|^2. \quad (29)$$

Furthermore, one can easily obtain $d\Gamma/dM_{\bar{K}^0 K^+}$, $d\Gamma/dM_{\bar{K}^0 \rho^-}$, and $d\Gamma/dM_{K^+ \rho^-}$ by integrating over each of the invariant mass variables with the limits of the Dalitz plot given in the RPP [28]. However, since the final meson ρ^- has a large width (~ 149.1 MeV), and the $K_1(1270)$ mass is very close to the $K\rho$ threshold (as shown by Fig. 4), one needs to take into account its finite width by folding with the vector-meson ρ^- spectral function for the invariant mass distributions [48], as follows,

$$\frac{d\tilde{\Gamma}}{dM_{12}} = \int_{m_{\rho^-} - 2\Gamma_{\rho^-}}^{m_{\rho^-} + 2\Gamma_{\rho^-}} d\hat{m}_{\rho^-} \left[\frac{d\Gamma}{dM_{12}} \times \omega(\hat{m}_{\rho^-}^2) \right], \quad (30)$$

where the mass m_{ρ^-} in $d\Gamma/dM_{12}$ should be replaced by \hat{m}_{ρ^-} . For example, the differential width $d\tilde{\Gamma}/dM_{\bar{K}^0 K^+}$ of the process $J/\psi \rightarrow \bar{K}^0 K^+ \rho^-$ becomes,

$$\begin{aligned} \frac{d\tilde{\Gamma}}{dM_{\bar{K}^0 K^+}} &= \int_{m_{\rho^-} - 2\Gamma_{\rho^-}}^{\min(m_{\rho^-} + 2\Gamma_{\rho^-}, m_{J/\psi} - M_{\bar{K}^0 K^+})} d\hat{m}_{\rho^-} \\ &\times \int_{M_{K^+ \rho^-}^{\min}}^{M_{K^+ \rho^-}^{\max}} dM_{K^+ \rho^-} \\ &\times \frac{M_{\bar{K}^0 K^+} M_{K^+ \rho^-}}{128\pi^3 m_{J/\psi}^3} |\mathcal{M}|^2 \times \omega(\hat{m}_{\rho^-}^2), \end{aligned} \quad (31)$$

where the range of $M_{\bar{K}^0 K^+}$ is,

$$m_{\bar{K}^0} + m_{K^+} < M_{\bar{K}^0 K^+} < m_{J/\psi} - m_{\rho^-} + 2\Gamma_{\rho^-}, \quad (32)$$

and the upper and lower limits for $M_{K^+ \rho^-}$ are,

$$\begin{aligned} (M_{K^+ \rho^-}^{\max})^2 &= (E_{K^+}^* + E_{\rho^-}^*)^2 - \\ &\quad \left(\sqrt{E_{K^+}^{*2} - m_{K^+}^2} - \sqrt{E_{\rho^-}^{*2} - \hat{m}_{\rho^-}^2} \right)^2 \\ (M_{K^+ \rho^-}^{\min})^2 &= (E_{K^+}^* + E_{\rho^-}^*)^2 - \\ &\quad \left(\sqrt{E_{K^+}^{*2} - m_{K^+}^2} + \sqrt{E_{\rho^-}^{*2} - \hat{m}_{\rho^-}^2} \right)^2, \end{aligned}$$

where $E_{K^+}^*$ and $E_{\rho^-}^*$ are the energies of K^+ and ρ^- in the $\bar{K}^0 \rho^-$ rest frame, respectively,

$$\begin{aligned} E_{K^+}^* &= \frac{M_{\bar{K}^0 K^+}^2 - m_{\bar{K}^0}^2 + m_{K^+}^2}{2M_{\bar{K}^0 K^+}}, \\ E_{\rho^-}^* &= \frac{m_{J/\psi}^2 - M_{\bar{K}^0 K^+}^2 - \hat{m}_{\rho^-}^2}{2M_{\bar{K}^0 K^+}}. \end{aligned} \quad (33)$$

III. RESULTS AND DISCUSSION

In our formalism, there are two unknown parameters: V_p for the weight of the $a_0(1710)$ contribution and V'_p for the one of the intermediate $K_1(1270)$ and $a_0(980)$ contributions. Since there are some similarities between the processes $J/\psi \rightarrow VVV$ and $J/\psi \rightarrow VPP$, it is expected that V_p and V'_p are of the same order of magnitude. Thus, we first take $V_p = V'_p$ and discuss the influence on our results of different values of V_p and V'_p .

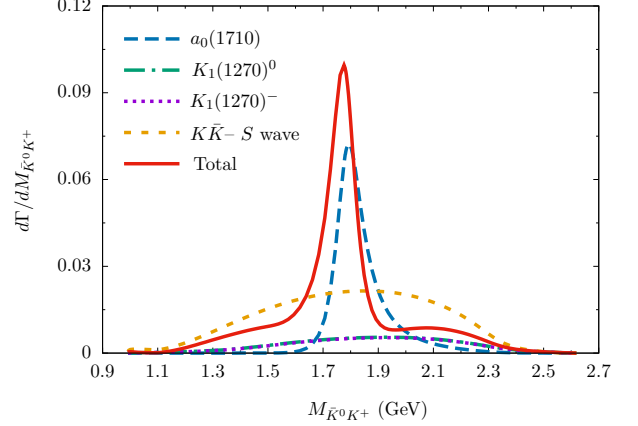


FIG. 9. $\bar{K}^0 K^+$ invariant mass distribution of the process $J/\psi \rightarrow \bar{K}^0 K^+ \rho^-$. The results are obtained with Eq. (30), where the width of final ρ^- is considered. The red-solid curve stands for the total contribution, while the blue-dashed curve, the green-dot-dashed curve, purple-dotted curve, and orange dashed curve correspond to the contributions from the $a_0(1710)$ state, the intermediate $K_1(1270)^0$, $K_1(1270)^-$, and the one from the direction production and the S -wave $K\bar{K}$ interaction of Eq. (20), respectively.

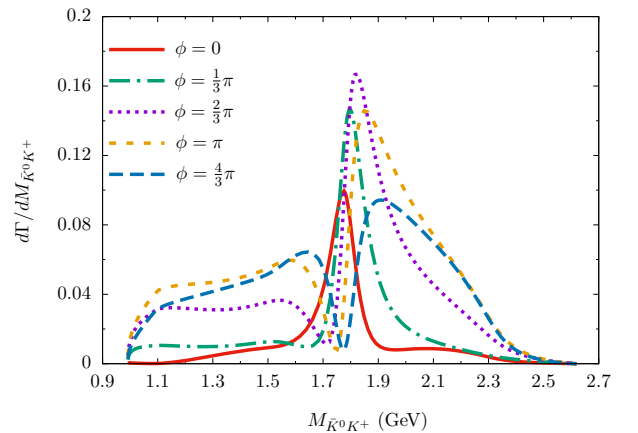


FIG. 10. $\bar{K}^0 K^+$ invariant mass distribution of the process $J/\psi \rightarrow \bar{K}^0 K^+ \rho^-$ obtained with a phase angle $\phi = 0, \pi/3, 2\pi/3, \pi$, and $4\pi/3$, respectively. See the text for details.

In Fig. 9, we show the $\bar{K}^0 K^+$ invariant mass distribu-

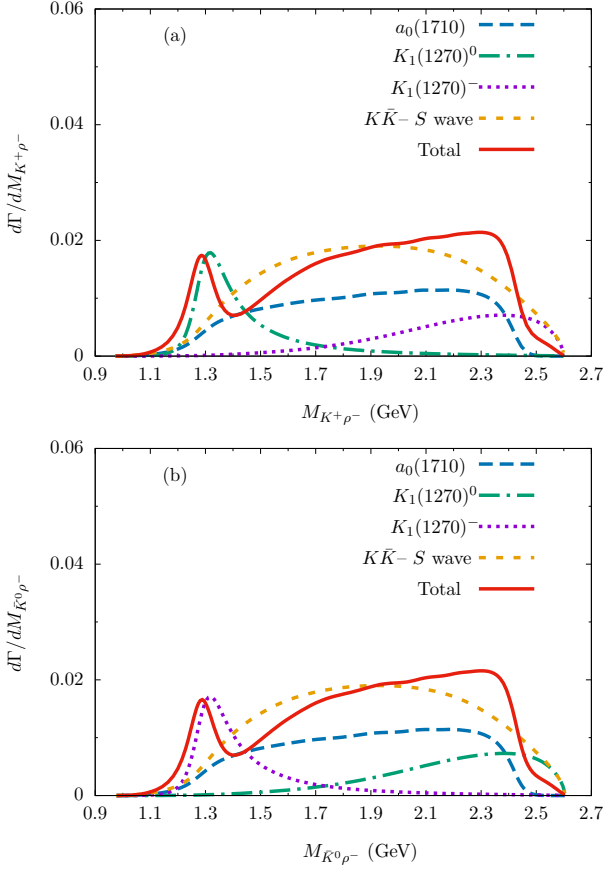


FIG. 11. (a) $K^+ \rho^-$ and (b) $\bar{K}^0 \rho^-$ invariant mass distributions of the process $J/\psi \rightarrow \bar{K}^0 K^+ \rho^-$. The explanations of the curves are the same as those of Fig. 9.

tion of the process $J/\psi \rightarrow \bar{K}^0 K^+ \rho^-$. The red-solid curve stands for the total contributions from the $a_0(1710)$ state, the axial-vector $K_1(1270)$ meson, and the S wave $\bar{K}K$ interaction, while the blue-dashed curve corresponds to the contribution from the $a_0(1710)$ state. Moreover, the green-dot-dashed and purple-dotted curves correspond to the contributions from the intermediate $K_1(1270)^0$ and $K_1(1270)^-$, respectively, and orange dashed curve corresponds to the contributions from the direction production and the S -wave $K\bar{K}$ interaction of Eq. (20). One can find a clear peak structure around 1.8 GeV, which could be associated with the scalar $a_0(1710)$. However, there is no significant structure of the $a_0(980)$ near the $\bar{K}^0 K^+$ threshold, because of the suppression by the phase space. The intermediate resonances $K_1(1270)^0$ and $K_1(1270)^-$ give the smooth contributions in the region of $1.4 \sim 2.4$ GeV, which is due to the fact that the $K_1(1270)$ couples to $K\rho$ in the S wave.

However, it should be pointed out that the peak structure appearing in the $\bar{K}^0 K^+$ invariant mass distribution of Fig. 9 could also manifest itself as a dip structure if the interference between $\mathcal{M}_a, \mathcal{M}_b, \mathcal{M}_c$, and \mathcal{M}_d is different from our naive assignments explained above. For instance, if we multiply the contribution of tree diagram

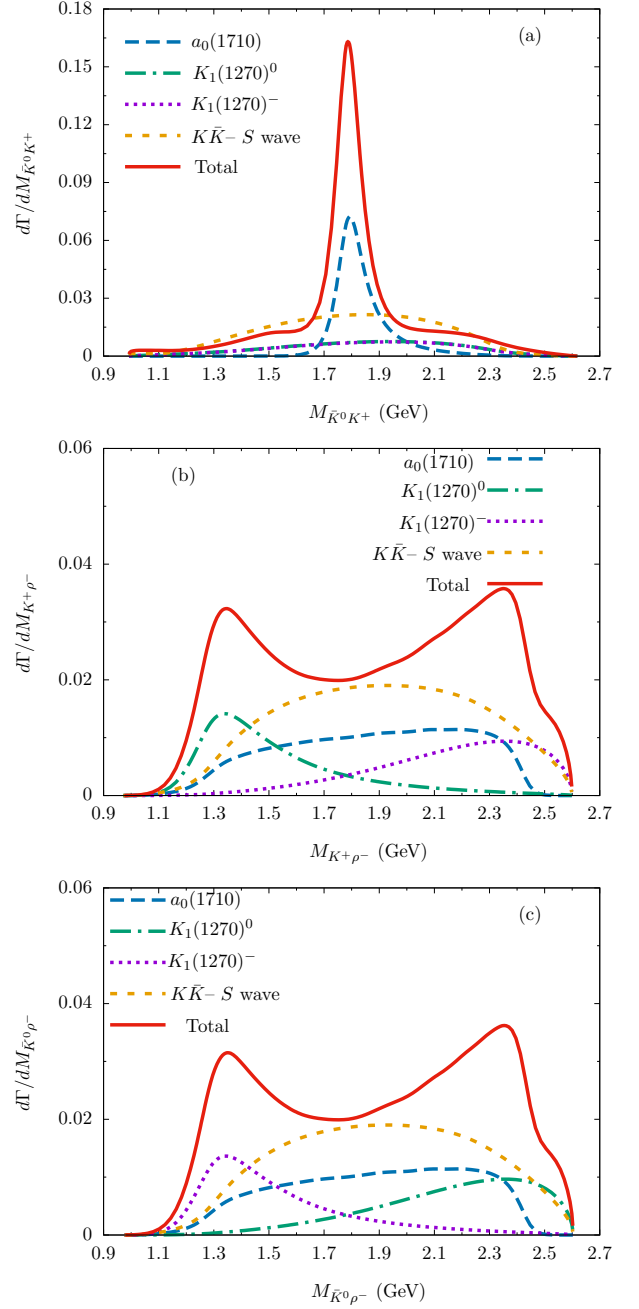


FIG. 12. The (a) $\bar{K}^0 K^+$, (b) $K^+ \rho^-$ and (c) $\bar{K}^0 \rho^-$ invariant mass distributions of the process $J/\psi \rightarrow \bar{K}^0 K^+ \rho^-$ with the parameters of lower pole of $K_1(1270)$. The explanations of the curves are the same as those of Fig. 9.

“1” of the term \mathcal{M}_d of of Eq. (27) by a phase factor $e^{i\phi}$ with $\phi = 0, \pi/3, 2\pi/3, \pi$, and $4\pi/3$, we would obtain the $\bar{K}^0 K^+$ invariant mass distribution shown in Fig. 10, where one can see a dip structure around 1.8 GeV for $\phi = 4\pi/3$.

Next, we have predicted the $K^+ \rho^-$ and $\bar{K}^0 \rho^-$ invariant mass distributions of the process $J/\psi \rightarrow \bar{K}^0 K^+ \rho^-$ in Figs. 11(a) and 11(b), respectively. One can see the clear

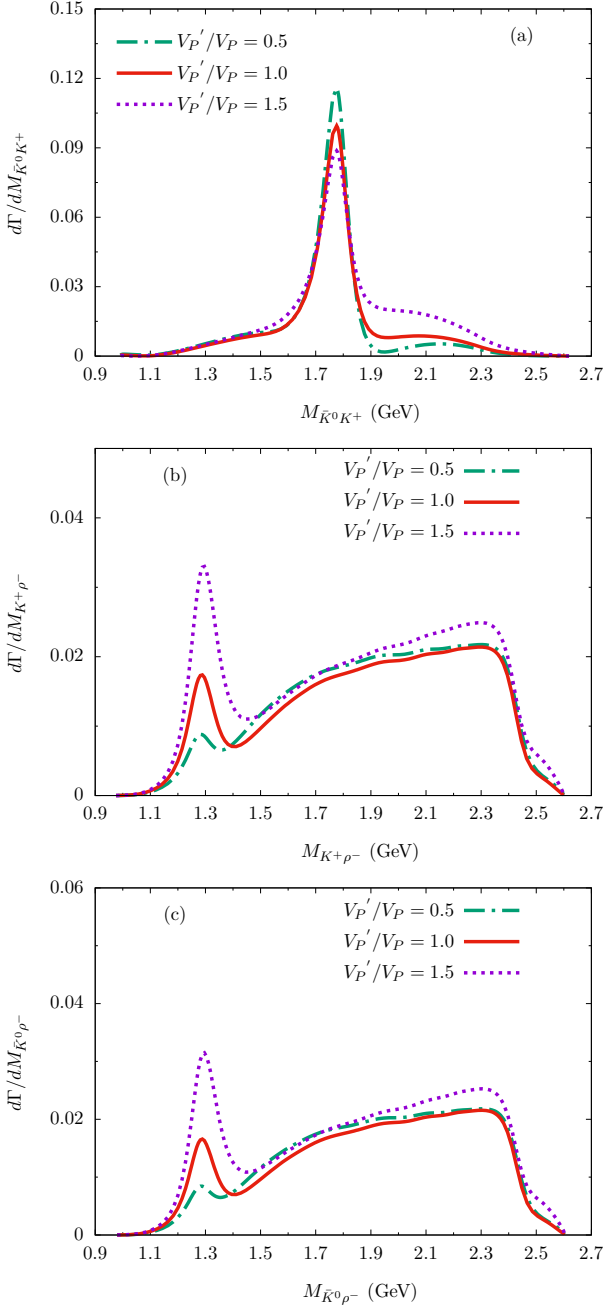


FIG. 13. (a) $\bar{K}^0 K^+$, (b) $K^+ \rho^-$, and (c) $\bar{K}^0 \rho^-$ invariant mass distributions of the process $J/\psi \rightarrow \bar{K}^0 K^+ \rho^-$ with $V_p'/V_p = 0.5, 1.0, 1.5$.

peaks of the $K_1(1270)^0$ and $K_1(1270)^-$ around 1.3 GeV. It should be stressed that the axial vector $K_1(1270)$ is predicted to have a two-pole structure, the lower pole is around 1200 MeV, coupled strongly to the $K^* \pi$ channel, and the higher pole is around 1280 MeV, coupled strongly to the $K \rho$ channels [46].

As we discussed above, since the higher pole of $K_1(1270)$ mainly couples to the $K \rho$ channel, we have adopted the pole position and coupling constant of the

higher pole in Eq. (19). To show the difference between the two poles of the $K_1(1270)$, we have calculated the $\bar{K}^0 K^+$, $K^+ \rho^-$, and $\bar{K}^0 \rho^-$ invariant mass distributions for the process $J/\psi \rightarrow \bar{K}^0 K^+ \rho^-$ with the pole position and coupling constant of the lower pole of Table IV in Eq. (19), as shown in Fig. 12. Because the coupling of the lower pole to $K \rho$ is smaller and the width is larger, the contribution from the lower pole of the $K_1(1270)$ is very small. For the contributions from the lower pole and the higher pole to have the same order of magnitude, we take $V_p'/V_p = 8.0$ in the results of Fig. 12. In the $\bar{K}^0 K^+$ invariant mass distribution of Fig. 12(a), one can find the clear peak structure around 1.8 GeV. However, in the $\bar{K}^0 \rho^-$ and $K^+ \rho^-$ invariant mass distributions of Figs. 12(b) and 12(c), only an enhancement structure appears. Thus, future measurements of $\bar{K}^0 \rho^-$ and $K^+ \rho^-$ invariant mass distributions could shed light on the two-pole structure of the $K_1(1270)$.

In addition, we take different ratios of $V_p'/V_p = 0.5, 1.0$, and 1.5 , and show the $\bar{K}^0 K^+$, $K^+ \rho^-$, and $\bar{K}^0 \rho^-$ invariant mass distributions for the process $J/\psi \rightarrow \bar{K}^0 K^+ \rho^-$ in Figs. 13(a)-13(c), respectively. One can find that the peak structure of the $a_0(1710)$ in the $\bar{K}^0 K^+$ invariant mass distribution remains similar for different values of V_p'/V_p , and the peak structures of the $K_1(1270)$ become clearer for larger values of V_p'/V_p .

IV. SUMMARY

Assuming the $a_0(1710)$ as a $K^* \bar{K}^*$ molecular state, we have investigated the process $J/\psi \rightarrow \bar{K}^0 K^+ \rho^-$ by taking into account the contribution from the S -wave $\omega \rho$, $K^* \bar{K}^*$, and $\phi \rho$ interactions, as well as the contribution from the intermediate resonances $a_0(980)$ and $K_1(1270)$.

We have predicted one peak structure around 1.8 GeV in the $\bar{K}^0 K^+$ invariant mass distribution, which could be associated with the scalar meson $a_0(1710)$. However, there is no significant near-threshold enhancement structure of the $a_0(980)$ in the $K \bar{K}$ invariant mass distribution. Furthermore, we have also predicted the $K^+ \rho^-$ and $\bar{K}^0 \rho^-$ invariant mass distributions of the process $J/\psi \rightarrow \bar{K}^0 K^+ \rho^-$, and find clear peaks of the resonance $K_1(1270)^{0,-}$. Considering the two-pole structure of the $K_1(1270)$, we have also calculated the results adopting parameters of the lower pole and find an enhancement structure near 1.3 GeV in the $K^+ \rho^-$ and $\bar{K}^0 \rho^-$ invariant mass distributions, which implies that future measurements of the $K^+ \rho^-$ and $\bar{K}^0 \rho^-$ invariant mass distributions could shed light on the two-pole structure of the $K_1(1270)$.

Finally, considering different weights ratio $V_p'/V_p = 0.5, 1.0$, and 1.5 of contributions from $a_0(1710)$ and $K_1(1270)$, we have shown the $\bar{K}^0 K^+$, $K^+ \rho^-$ and $\bar{K}^0 \rho^-$ invariant mass distributions of the process $J/\psi \rightarrow \bar{K}^0 K^+ \rho^-$, and find that the peak structure of $a_0(1710)$ remains essentially the same. We hope that our theoretical predictions could be tested by the BESIII and Belle

II experiments and the planned STCF in the future, and precise measurements of the process $J/\psi \rightarrow \bar{K}^0 K^+ \rho^-$ could shed light on the nature of the scalar $a_0(1710)$ and the axial vector $K_1(1270)$.

ACKNOWLEDGMENTS

L.S.G and J.J.X acknowledge support from the National Key R&D Program of China under Grant No. 2023YFA1606700. This work is supported by the Natural Science Foundation of Henan under Grant No.

222300420554 and No. 232300421140. This work is partly supported by the National Natural Science Foundation of China under Grants Nos. 12075288, 11975041, 11961141004, 12361141819, and 12192263, the Project of Youth Backbone Teachers of Colleges and Universities of Henan Province (2020GGJS017), the Open Project of Guangxi Key Laboratory of Nuclear Physics and Nuclear Technology, No. NLK2021-08, and the Central Government Guidance Funds for Local Scientific and Technological Development, China (No. Guike ZY22096024). It is also partly supported by the Youth Innovation Promotion Association CAS.

-
- [1] H. X. Chen, W. Chen, X. Liu, Y. R. Liu and S. L. Zhu, Rept. Prog. Phys. **80**, no.7, 076201 (2017) doi:10.1088/1361-6633/aa6420 [arXiv:1609.08928 [hep-ph]].
 - [2] H. X. Chen, W. Chen, X. Liu, Y. R. Liu and S. L. Zhu, Rept. Prog. Phys. **86** (2023) no.2, 026201 doi:10.1088/1361-6633/aca3b6 [arXiv:2204.02649 [hep-ph]].
 - [3] E. Oset, W. H. Liang, M. Bayar, J. J. Xie, L. R. Dai, M. Albaladejo, M. Nielsen, T. Sekihara, F. Navarra and L. Roca, *et al.* Int. J. Mod. Phys. E **25** (2016), 1630001 doi:10.1142/S0218301316300010 [arXiv:1601.03972 [hep-ph]].
 - [4] M. Z. Liu, Y. W. Pan, Z. W. Liu, T. W. Wu, J. X. Lu and L. S. Geng, [arXiv:2404.06399 [hep-ph]].
 - [5] H. Y. Gao and B. Q. Ma, Mod. Phys. Lett. A **14** (1999), 2313-2319 doi:10.1142/S021773239900239X [arXiv:hep-ph/0305294 [hep-ph]].
 - [6] F. K. Guo, C. Hanhart, U. G. Meißner, Q. Wang, Q. Zhao and B. S. Zou, Rev. Mod. Phys. **90** (2018) no.1, 015004 [erratum: Rev. Mod. Phys. **94** (2022) no.2, 029901] doi:10.1103/RevModPhys.90.015004 [arXiv:1705.00141 [hep-ph]].
 - [7] E. Wang, L. S. Geng, J. J. Wu, J. J. Xie and B. S. Zou, [arXiv:2406.07839 [hep-ph]].
 - [8] J. P. Lees *et al.* [BaBar], Phys. Rev. D **104** (2021) no.7, 072002 doi:10.1103/PhysRevD.104.072002 [arXiv:2106.05157 [hep-ex]].
 - [9] M. Ablikim *et al.* [BESIII], Phys. Rev. D **105** (2022) no.5, L051103 doi:10.1103/PhysRevD.105.L051103 [arXiv:2110.07650 [hep-ex]].
 - [10] M. Ablikim *et al.* [BESIII], Phys. Rev. Lett. **129** (2022) no.18, 18 doi:10.1103/PhysRevLett.129.182001 [arXiv:2204.09614 [hep-ex]].
 - [11] H. Nagahiro, L. Roca, E. Oset and B. S. Zou, Phys. Rev. D **78** (2008), 014012 doi:10.1103/PhysRevD.78.014012 [arXiv:0803.4460 [hep-ph]].
 - [12] T. Branz, L. S. Geng and E. Oset, Phys. Rev. D **81** (2010), 054037 doi:10.1103/PhysRevD.81.054037 [arXiv:0911.0206 [hep-ph]].
 - [13] L. S. Geng, F. K. Guo, C. Hanhart, R. Molina, E. Oset and B. S. Zou, Eur. Phys. J. A **44** (2010), 305-311 doi:10.1140/epja/i2010-10971-5 [arXiv:0910.5192 [hep-ph]].
 - [14] J. J. Xie and E. Oset, Phys. Rev. D **90** (2014) no.9, 094006 doi:10.1103/PhysRevD.90.094006 [arXiv:1409.1341 [hep-ph]].
 - [15] A. Martinez Torres, K. P. Khemchandani, F. S. Navarra, M. Nielsen and E. Oset, Phys. Lett. B **719** (2013), 388-393 doi:10.1016/j.physletb.2013.01.036 [arXiv:1210.6392 [hep-ph]].
 - [16] Z. L. Wang and B. S. Zou, Phys. Rev. D **104** (2021) no.11, 114001 doi:10.1103/PhysRevD.104.114001 [arXiv:2107.14470 [hep-ph]].
 - [17] C. Garcia-Recio, L. S. Geng, J. Nieves and L. L. Salcedo, Phys. Rev. D **83** (2011), 016007 doi:10.1103/PhysRevD.83.016007 [arXiv:1005.0956 [hep-ph]].
 - [18] C. García-Recio, L. S. Geng, J. Nieves, L. L. Salcedo, E. Wang and J. J. Xie, Phys. Rev. D **87** (2013) no.9, 096006 doi:10.1103/PhysRevD.87.096006 [arXiv:1304.1021 [hep-ph]].
 - [19] F. E. Close and Q. Zhao, Phys. Rev. D **71** (2005), 094022 doi:10.1103/PhysRevD.71.094022 [arXiv:hep-ph/0504043 [hep-ph]].
 - [20] L. C. Gui *et al.* [CLQCD], Phys. Rev. Lett. **110**, 021601 (2013). doi:10.1103/PhysRevLett.110.021601 [arXiv:1206.0125 [hep-lat]].
 - [21] S. Janowski, F. Giacosa and D. H. Rischke, Phys. Rev. D **90**, 114005 (2014). doi:10.1103/PhysRevD.90.114005 [arXiv:1408.4921 [hep-ph]].
 - [22] A. H. Fariborz, A. Azizi and A. Asrar, Phys. Rev. D **92**, 113003 (2015). doi:10.1103/PhysRevD.92.113003 [arXiv:1511.02449 [hep-ph]].
 - [23] Y. Chen, A. Alexandru, S. J. Dong, T. Draper, I. Horvath, F. X. Lee, K. F. Liu, N. Mathur, C. Morningstar and M. Peardon, *et al.* Phys. Rev. D **73** (2006), 014516 doi:10.1103/PhysRevD.73.014516 [arXiv:hep-lat/0510074 [hep-lat]]. Achasov:2023zoi, Achasov:2023izs
 - [24] N. N. Achasov and G. N. Shestakov, JETP Lett. **118** (2023) no.6, 385-386 doi:10.1134/S002136402360266X [arXiv:2307.03472 [hep-ph]].
 - [25] N. N. Achasov and G. N. Shestakov, Phys. Rev. D **108** (2023) no.3, 036018 doi:10.1103/PhysRevD.108.036018 [arXiv:2306.04478 [hep-ph]].
 - [26] L. S. Geng and E. Oset, Phys. Rev. D **79** (2009), 074009 doi:10.1103/PhysRevD.79.074009 [arXiv:0812.1199 [hep-ph]].
 - [27] M. L. Du, D. Gülmez, F. K. Guo, U. G. Meißner and Q. Wang, Eur. Phys. J. C **78** (2018) no.12, 988 doi:10.1140/epjc/s10052-018-6475-8 [arXiv:1808.09664 [hep-ph]].

- [28] R. L. Workman *et al.* [Particle Data Group], PTEP **2022** (2022), 083C01 doi:10.1093/ptep/ptac097
- [29] Z. L. Wang and B. S. Zou, Eur. Phys. J. C **82** (2022) no.6, 509 doi:10.1140/epjc/s10052-022-10460-4 [arXiv:2203.02899 [hep-ph]].
- [30] G. Y. Wang, S. C. Xue, G. N. Li, E. Wang and D. M. Li, Phys. Rev. D **97** (2018) no.3, 034030 doi:10.1103/PhysRevD.97.034030 [arXiv:1712.10180 [hep-ph]].
- [31] Q. H. Shen, X. Zhang, X. Liu and J. J. Xie, Phys. Rev. D **109** (2024) no.1, 014012 doi:10.1103/PhysRevD.109.014012 [arXiv:2310.07258 [hep-ph]].
- [32] D. Guo, W. Chen, H. X. Chen, X. Liu and S. L. Zhu, Phys. Rev. D **105** (2022) no.11, 114014 doi:10.1103/PhysRevD.105.114014 [arXiv:2204.13092 [hep-ph]].
- [33] M. Ablikim *et al.* [BES], Phys. Rev. Lett. **96** (2006), 162002 doi:10.1103/PhysRevLett.96.162002 [arXiv:hep-ex/0602031 [hep-ex]].
- [34] M. Ablikim *et al.* [BESIII], Phys. Rev. D **87** (2013) no.3, 032008 doi:10.1103/PhysRevD.87.032008 [arXiv:1211.5668 [hep-ex]].
- [35] X. Zhu, D. M. Li, E. Wang, L. S. Geng and J. J. Xie, Phys. Rev. D **105** (2022) no.11, 116010 doi:10.1103/PhysRevD.105.116010 [arXiv:2204.09384 [hep-ph]].
- [36] X. Zhu, H. N. Wang, D. M. Li, E. Wang, L. S. Geng and J. J. Xie, Phys. Rev. D **107** (2023) no.3, 034001 doi:10.1103/PhysRevD.107.034001 [arXiv:2210.12992 [hep-ph]].
- [37] L. R. Dai, E. Oset and L. S. Geng, Eur. Phys. J. C **82** (2022) no.3, 225 doi:10.1140/epjc/s10052-022-10178-3 [arXiv:2111.10230 [hep-ph]].
- [38] E. Oset, L. R. Dai and L. S. Geng, Sci. Bull. **68** (2023), 243-246 doi:10.1016/j.scib.2023.01.011 [arXiv:2301.08532 [hep-ph]].
- [39] Z. Y. Wang, Y. W. Peng, J. Y. Yi, W. C. Luo and C. W. Xiao, Phys. Rev. D **107** (2023) no.11, 116018 doi:10.1103/PhysRevD.107.116018
- [40] Y. Ding, X. H. Zhang, M. Y. Dai, E. Wang, D. M. Li, L. S. Geng and J. J. Xie, Phys. Rev. D **108**, no.11, 114004 (2023) doi:10.1103/PhysRevD.108.114004 [arXiv:2306.15964 [hep-ph]].
- [41] J. P. Lees *et al.* [BaBar], Phys. Rev. D **93** (2016), 012005 doi:10.1103/PhysRevD.93.012005 [arXiv:1511.02310 [hep-ex]].
- [42] X. Y. Wang, H. F. Zhou and X. Liu, Phys. Rev. D **108** (2023) no.3, 034015 doi:10.1103/PhysRevD.108.034015 [arXiv:2306.12815 [hep-ph]].
- [43] M. Ablikim *et al.* [BESIII], Chin. Phys. C **46** (2022) no.7, 074001 doi:10.1088/1674-1137/ac5c2e [arXiv:2111.07571 [hep-ex]].
- [44] M. Achasov, X. C. Ai, L. P. An, R. Aliberti, Q. An, X. Z. Bai, Y. Bai, O. Bakina, A. Barnyakov and V. Blinov, *et al.* Front. Phys. (Beijing) **19** (2024) no.1, 14701 doi:10.1007/s11467-023-1333-z [arXiv:2303.15790 [hep-ex]].
- [45] J. P. Lees *et al.* [BaBar], Phys. Rev. D **95** (2017) no.9, 092005 doi:10.1103/PhysRevD.95.092005 [arXiv:1704.05009 [hep-ex]].
- [46] L. S. Geng, E. Oset, L. Roca and J. A. Oller, Phys. Rev. D **75** (2007), 014017 doi:10.1103/PhysRevD.75.014017 [arXiv:hep-ph/0610217 [hep-ph]].
- [47] G. Y. Wang, L. Roca, E. Wang, W. H. Liang and E. Oset, Eur. Phys. J. C **80** (2020) no.5, 388 doi:10.1140/epjc/s10052-020-7939-1 [arXiv:2002.07610 [hep-ph]].
- [48] G. Y. Wang, L. Roca and E. Oset, Phys. Rev. D **100** (2019) no.7, 074018 doi:10.1103/PhysRevD.100.074018 [arXiv:1907.09188 [hep-ph]].
- [49] J. M. Xie, J. X. Lu, L. S. Geng and B. S. Zou, [arXiv:2312.17287 [hep-ph]].
- [50] J. M. Xie, J. X. Lu, L. S. Geng and B. S. Zou, Phys. Rev. D **108** (2023) no.11, L111502 doi:10.1103/PhysRevD.108.L111502 [arXiv:2307.11631 [hep-ph]].
- [51] S. Sakai, W. H. Liang, G. Toledo and E. Oset, Phys. Rev. D **101** (2020) no.1, 014005 doi:10.1103/PhysRevD.101.014005 [arXiv:1909.08888 [hep-ph]].
- [52] N. Ikeno, J. M. Dias, W. H. Liang and E. Oset, Phys. Rev. D **100** (2019) no.11, 114011 doi:10.1103/PhysRevD.100.114011 [arXiv:1909.11906 [hep-ph]].
- [53] S. J. Jiang, S. Sakai, W. H. Liang and E. Oset, Phys. Lett. B **797** (2019), 134831 doi:10.1016/j.physletb.2019.134831 [arXiv:1904.08271 [hep-ph]].
- [54] M. Y. Duan, G. Y. Wang, E. Wang, D. M. Li and D. Y. Chen, Phys. Rev. D **104** (2021) no.7, 074030 doi:10.1103/PhysRevD.104.074030 [arXiv:2109.00731 [hep-ph]].
- [55] L. M. Abreu, W. F. Wang and E. Oset, Eur. Phys. J. C **83** (2023) no.3, 243 doi:10.1140/epjc/s10052-023-11384-3 [arXiv:2301.08058 [hep-ph]].
- [56] R. Molina, L. R. Dai, L. S. Geng and E. Oset, Eur. Phys. J. A **56** (2020) no.6, 173 doi:10.1140/epja/s10050-020-00176-y [arXiv:1909.10764 [hep-ph]].
- [57] R. Molina, D. Nicmorus and E. Oset, Phys. Rev. D **78** (2008), 114018 doi:10.1103/PhysRevD.78.114018 [arXiv:0809.2233 [hep-ph]].
- [58] W. T. Lyu, Y. H. Lyu, M. Y. Duan, D. M. Li, D. Y. Chen and E. Wang, Phys. Rev. D **109** (2024) no.1, 014008 doi:10.1103/PhysRevD.109.014008 [arXiv:2306.16101 [hep-ph]].
- [59] M. Y. Duan, D. Y. Chen and E. Wang, Eur. Phys. J. C **82** (2022) no.10, 968 doi:10.1140/epjc/s10052-022-10948-z [arXiv:2207.03930 [hep-ph]].
- [60] L. S. Geng, E. Oset, R. Molina and D. Nicmorus, PoS **EFT09** (2009), 040 doi:10.22323/1.069.0040 [arXiv:0905.0419 [hep-ph]].
- [61] J. A. Oller and E. Oset, AIP Conf. Proc. **432** (1998) no.1, 824-827 doi:10.1063/1.55984 [arXiv:hep-ph/9710554 [hep-ph]].
- [62] J. A. Oller, E. Oset and J. R. Pelaez, Phys. Rev. D **59** (1999), 074001 [erratum: Phys. Rev. D **60** (1999), 099906; erratum: Phys. Rev. D **75** (2007), 099903] doi:10.1103/PhysRevD.59.074001 [arXiv:hep-ph/9804209 [hep-ph]].
- [63] J. A. Oller, E. Oset and J. R. Pelaez, Phys. Rev. Lett. **80** (1998), 3452-3455 doi:10.1103/PhysRevLett.80.3452 [arXiv:hep-ph/9803242 [hep-ph]].
- [64] X. C. Feng, L. L. Wei, M. Y. Duan, E. Wang and D. M. Li, Phys. Lett. B **846** (2023), 138185 doi:10.1016/j.physletb.2023.138185 [arXiv:2009.08600 [hep-ph]].
- [65] J. Y. Wang, M. Y. Duan, G. Y. Wang, D. M. Li, L. J. Liu and E. Wang, Phys. Lett. B **821** (2021), 136617

- doi:10.1016/j.physletb.2021.136617 [arXiv:2105.04907 [hep-ph]].
- [66] J. J. Xie, L. R. Dai and E. Oset, Phys. Lett. B **742** (2015), 363-369 doi:10.1016/j.physletb.2015.02.006 [arXiv:1409.0401 [hep-ph]].
- [67] X. Z. Ling, M. Z. Liu, J. X. Lu, L. S. Geng and J. J. Xie, Phys. Rev. D **103** (2021) no.11, 116016 doi:10.1103/PhysRevD.103.116016 [arXiv:2102.05349 [hep-ph]].
- [68] M. Y. Duan, J. Y. Wang, G. Y. Wang, E. Wang and D. M. Li, Eur. Phys. J. C **80** (2020) no.11, 1041 doi:10.1140/epjc/s10052-020-08630-3 [arXiv:2008.10139 [hep-ph]].
- [69] V. R. Debastiani, W. H. Liang, J. J. Xie and E. Oset, Phys. Lett. B **766** (2017), 59-64 doi:10.1016/j.physletb.2016.12.054 [arXiv:1609.09201 [hep-ph]].